International Journal of Advanced Science and Research
ISSN: 2455-4227
Impact Factor: RJIF 5.12
www.allsciencejournal.com
Volume 2; Issue 5; September 2017; Page No. 06-10

To study the ESR spectrum of natural wollastonite

[1] Arvinder Singh, [2] Dr. Manoj S Shekhawat
[1] Vill & P.O. Daburji, Dist. Kapurthala, Punjab, India
[2] Dept. of Physics, Govt. Engg. College, New Delhi, India

Abstract
The ESR spectrum of natural wollastonite has a strong angular dependence that we interpret as originating from Mn^{2+}ions distributed among the 6-coordinated Ca sites (Cal, Ca2) and the 7-coordinated Ca site (Ca3). A computer fit to the spectrum shows superposition of spectra from Mn^{2+} ions in two magnetically nonequivalent kinds of sites with the Hamiltonian parameters $g_1 = g_2 = 2.002$, $A_1 = A_2 = 85$ cm^{-1} D, = $D_2 = -357$ cm^{-1} and $E_1 = E_2 = 90$ cm^{-1}; and $g_3 = 1.998$, $A_3 = 87$ cm^{-1},$D_3 = -231$ cm^{-1}, and $E_3 = 19$ cm^{-1} with subscripts referring to the sites Cal, Ca2 and Ca3, respectively. A crystal-field calculation gives zero-field splitting ratios of $|E_1/D_1| = |E_2/D_2| = 0.25$ and $|E_3/D_3| =$ for the two signals, compared with the experimentally measured ratios $|E_1/D_1| = 0.15$ and $|E_3/D_3| = 0.12$. We interpret these signals as arising from Mn^{2+} on the 6-coordinated Ca sites (Cal, Ca2) and the 7-coordinated Ca site (Ca3).

Keywords: ESR spectrum, wollastonite and hamiltonian parameters

Introduction
Wollastonite is a calcium metasilicate with the nominal formula $CaSiO_3$, which occurs in tabular crystals elongated parallel to the *b* axis. It is used in the ceramic industry as the main ingredient in single-fired wall tile and as an accessory additive in several types of ceramic bodies and glazes. It is also an important mineral in high- grade metamorphic rocks (Ladoo, 1937) [5].
In natural minerals like wollastonite Mn^{2+} often substitutes for Ca^{2t}. The Mn^{2+} is paramagnetic and hence favorable for study by electron-spin-resonance (ESR). In this article we present the results of such a study and interpret them in terms of the local crystal environment.

Crystal Structure
The crystal structure of wollastonite was determined by Mamedov and Belov (1956) [6] and refined by Buerger and Prewitt (1961), who found that it crystallizes in the triclinic space group $P\bar{1}$, C_i^1 with six $CaSiO_3$ per unit cell, and *a* = 7.94 A, *b* = 7.32 A, *c* = 7.07 A, α = 90°02', β = 95°22', and γ = l03°26'. Peacor and Prewitt (1963) gave an excellent discussion of the crystal structure of wollastonite in comparison with that of bustamite.
The arrangement of the oxygen atoms approximates close packing with layering parallel to (101). Layers composed of Ca atoms in octahedral coordination alternate with layers consisting of Si atoms between the sheets of oxygen atoms. The SiO_4tetrahedra are ordered in chains which have a repeat unit of three tetrahedra and which are oriented parallel to the b axis. Two of the Ca atoms are octahedrally coordinated with Ca-O distances ranging from 2.272 to 2.548 A and an average value of 2.387.
The other Ca, Ca3, is 7-coordinated, with the seventh oxygen at a distance of 2.642 A.

Chemical Analysis and X-Ray Results
The sample under study originated in Payande, Departamento del Tolima, Colombia. The results of the chemical and atomic spectroscopic analysis done by el Instituto nacional de investiga ciones geologic mineras de Bogota is presented in Table 1. These results indicate that the sample is 78.6% wollastonite, 5.7% calcite, and 5.5% dolomite. There is one Mn atom for every 146 Ca atoms. Powder X-ray diffraction confirms the identity of wollastonite as the principal constituent of this sample.

Experimental Methods
The Mn^{2+} ion is in the $^6S_{5/2}$ spectroscopic state, which is paramagnetic and can be detected by the technique of electron-spin resonance. Since its orbital magnetic moment is zero (*L* = 0), its ESR spectrum appears at a g factor close to 2.00. To obtain this spectrum, the sample was placed in a high-Q microwave-resonant cavity oscillating at 9.3 GHz, and the magnetic field was scanned through the region near g = 2.00 to detect the resonant absorption due to the precession of the unpaired spins in the field. A Varian E-line spectrometer equipped with a tracor Northern signal processor was used to make this measurement. The spectrum consists of many lines owing to the multiplicity of energy levels arising from the electronic spin S and from the nuclear spin *I*. The positions of these lines were measured for a series of orientations of the sample relative to the applied magnetic field. The directions of the applied field relative to the orientations of the oxygen ions surrounding the Mn^{2+} ions determine the details of each spectrum. Each Ca site gives rise to a characteristic spectrum for the Mn^{2+} substituted there.

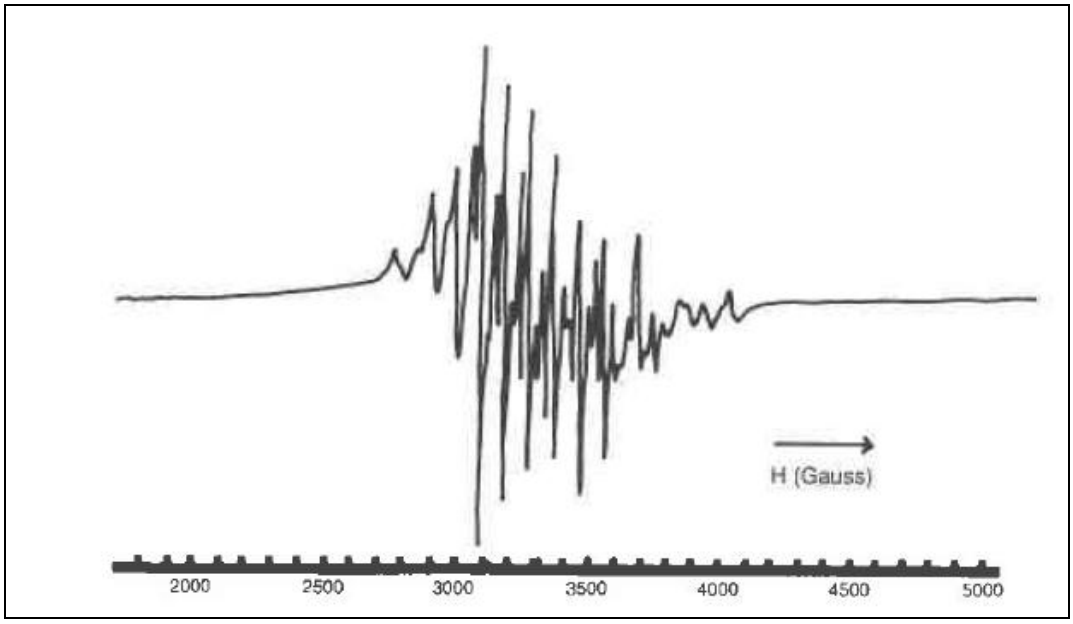

Fig 1: Typical ESR spectrum of Mn^{2+} in wollastonite, showing the first derivative of the absorption (in arbitrary units) plotted against the scanning magnetic field strength in the range from 1200 G to 5200 G. The magnetic field range over which absorption occurs is fairly narrow for this orientation of the sample.

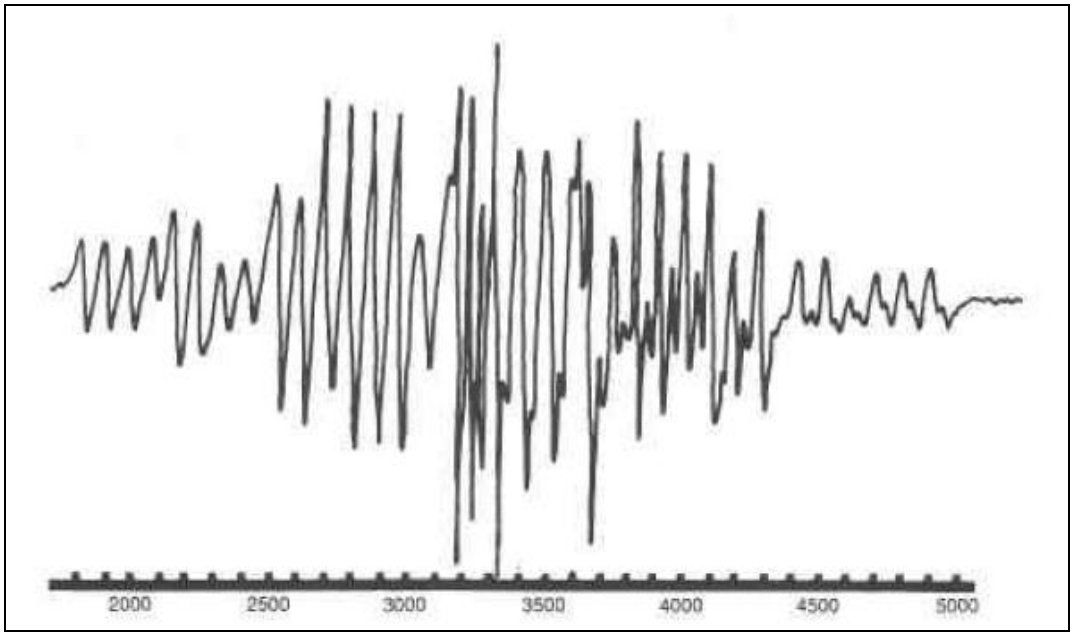

Fig 2: ESR spectrum of Mn^{2+}after a crystal rotation of 110º with respect to that of Fig. 1. The range of absorption is much greater for this orientation of the sample.

Theory

Mn^{2+} has five electrons that give it an electronic spin of 5/2, as was mentioned above, and the crystalline electric field caused by the surrounding oxygen's splits the S = 5/2 energy state into three doublet levels, with the magnetic spin quantum numbers M = ± 5/2, ±3/2 and ± 1/2. This electronic spin S interacts with the applied magnetic field H to separate the +M and -M levels of each pair and to move these six levels farther apart. The electronic spin S also interacts with the nuclear spin I = 5/2 of the Mn nucleus to split each M level into six m levels arising from the six values of the nuclear spin quantum number *m* = ± 5/2, ± 3/2, ± 1/2. These factors result in a total of 36 energy levels. An additional small splitting due to the interaction of the nuclear spin with the applied magnetic field is neglected.

The energy states of the system are described by the following spin Hamiltonian:

$$H = g\mu_B \vec{H}.\vec{S} + A\vec{S}.\vec{I} + D[S_Z^2 - (1/3)S(S+1)] + E[S_x^2 - S_y^2],$$

where the Zeeman term $g\mu_B \vec{H}.\vec{S}$ is the interaction of the electronic spin with the magnetic field, and hyperfine term $A\vec{S}.\vec{I}$ is the electron-spin—nuclear-spin interaction, and there

are two so-called zero-field terms, namely *D*, representing the axial part, and *E*, due to the deviation from axial symmetry. As the magnetic field is scanned, only certain transitions are observed owing to the restrictions imposed by the selection rules.

Since the selection rules for paramagnetic resonance, $\Delta M = \pm 1$ and $\Delta m = 0$, allow *M* to change by 1, the ESR spectrum is expected to split into five fine-structure transitions, each of which should split into six hyperfine components. Here *M* and *m* respectively are the values of the electronic- and nuclear-spin component along the direction of the field. In general, there are 30 ΔM = ±1, Δm= 0 allowed transitions and many more ΔM = ±1, Δm = ±1, or ΔM = ±1, Δm = ± 2 forbidden transitions for each magnetically nonequivalent Mn^{2+}cation.

ESR Results

Figures 1 and 2 shows the spectrum of Mn^{2+} for two different orientations of the magnetic field. Figure 2 gives the spectrum with the maximum spread. Many of the 30 lines are doubled, especially those on the right side and in the center of the spectrum. Thus, the number of lines is greater than expected for single Mn^{2+} sites, indicating that there is more than one nonequivalent Mn^{2+} site. The nonequivalence could be due to different surroundings or different orientations. The spectrum was recorded at 15° intervals around three perpendicular axes. Careful observation of these spectra, especially those with maximum spread led to the conclusion that the observed spectra are super positions arising from Mn^{2+} located on two different sites with different fine-structure parameters.

Crystal-Field Analysis

In wollastonite, Mn^{2+} is expected to substitute for Ca, in three Ca sites (Cal, Ca2, and Ca3). Atoms Cal and Ca2 are 6-coordinated with an average Ca-O interatomic distance of 2.38 A Ca3 is 7-coordinated with interatomic distances between 2.335 and 2.642 A. The large value (2.642) corresponds to Ca3-09 and the average interatomic distance 2.39 A.

Table 1: Chemical analysis (%) of wollastonite sample

CaO	44.80
SiO^2	40.66
CO_2	5.16
MgO	1.66
Fe_2O_3	0.70
MnO	0.42
K_2O	0.02
Na_2O	0.01
Al_2O_3	0.00
NiO	0.00
TiO_2	0.00

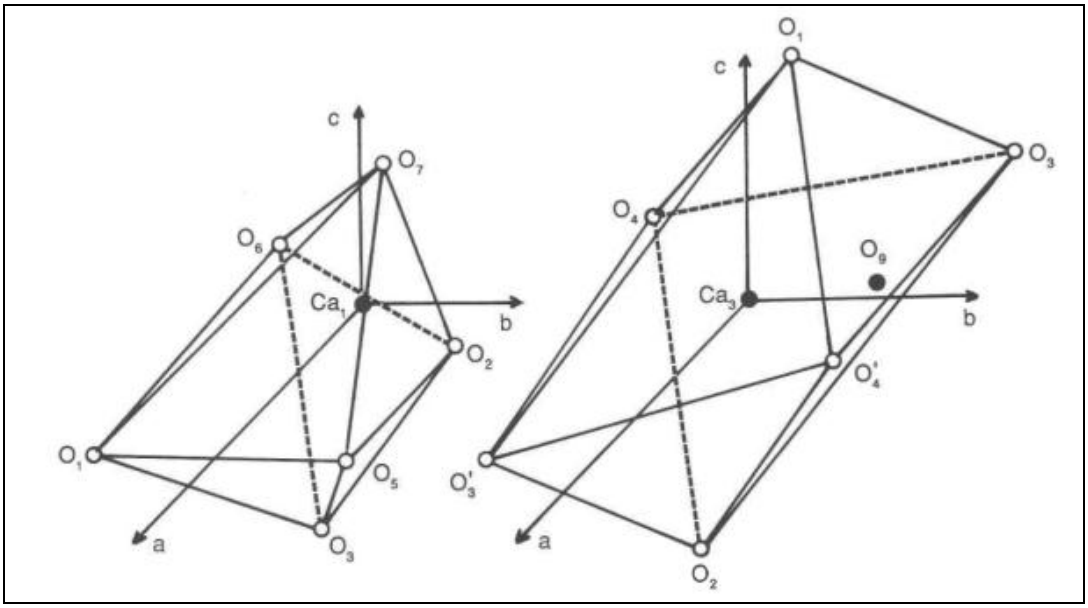

Fig 3: Arrangement of nearest-neighbor oxygen atoms around the calcium ions in sites (a) Cal and (b) Ca3. The former has six and the latter seven oxygen nearest-neighbors. Calcium site Ca2 is similar to Cal.

The crystal-field potentials of the 6-coordinated sites Cal and Ca2 are quite similar, whereas that at Ca3 is different because the additional oxygen 09 is present and because the octahedral coordination of ligand oxygen atoms is distorted differently (Fig. 3). The schemes of Figure 3 were obtained after a coordinate transformation given by

$$\begin{bmatrix} a \\ b \\ c \end{bmatrix} = \begin{bmatrix} 1 & \cos 103.43^\circ & \cos 95.37^\circ \\ 0 & \cos 13.43^\circ & \cos 91.28^\circ \\ 0 & 0 & \cos 5.52^\circ \end{bmatrix} \begin{bmatrix} a' \\ b' \\ c' \end{bmatrix}$$

where (*a,' b', c'*) is the triclinic system of the unit cell of wollastonite and (*a, b, c*) is an orthogonal cartesian system with *a, a'* coincident and *b*' in the *a*, *b* plane.

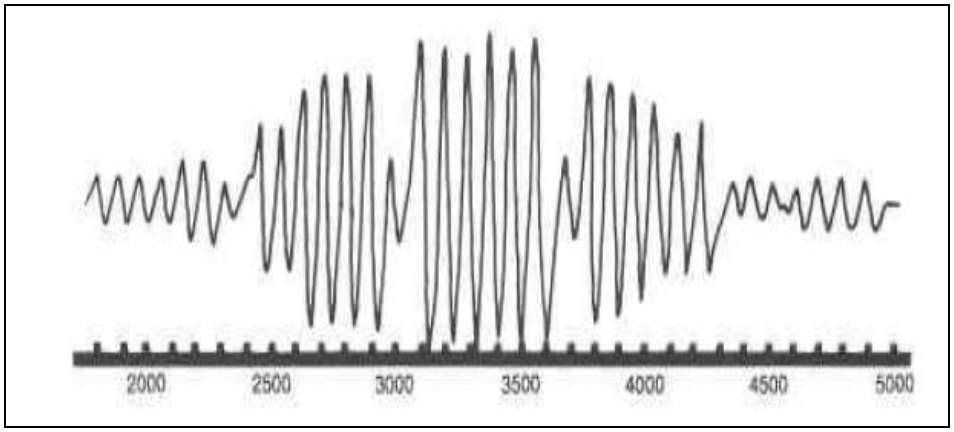

Fig 4: Calculated ESR spectrum of Mn^{2+} in wollastonite. The five sets of six lines are evident. This spectrum is for a single site, whereas the experimental spectra of Figs. 1 and 2 are super positions of spectra from more than one site.

With the aid of the spherical harmonic addition theorem, the crystalline field potential can be written in a general and practical form as

$$V = \sum A_l^m \langle r \rangle Y_l^m = \sum B_l^m Y_l^m, \quad (3)$$

Where, the $A^m{}_l$ values are constants determined by the characteristics of the charge distribution, $\langle r \rangle$ is the mean value of the lth power of the electron wave-function radius, and $Y^m{}_l$ are the spherical harmonic functions that take account of the angular dependence on the potential.

Table 2: Oxygen coordinates and Ca-O distances *R* for Ca-O Octahedra

Octahedron	Atom	X (A)	Y(A)	Z(A)	R(A)
(Ca1)O6	O1	2.13	-1.37	0.29	2.55
	O2	1.05	2.15	0.49	2.44
	O3	0.96	0.34	-2.09	2.32
	O5	-1.78	1.45	-0.19	2.30
	O6	-0.93	-2.07	-0.18	2.27
	O7	0.22	0.58	2.33	2.41
(Ca2)O6	O1	1.26	2.14	0.27	2.50
	O2	1.87	-1.46	0.47	2.42
	O4	0.97	0.10	-2.10	2.32
	O5	-0.95	-2.16	-0.21	2.37
	O6	-1.80	1.45	-0.20	2.32
	O8	0.42	-0.46	2.32	2.41
(Ca3)O7	O1	-0.72	-0.18	2.32	2.44
	O2	0.97	0.22	-2.13	2.35
	O3	-1.89	1.52	-0.06	2.43
	O'3	1.86	-1.34	0.45	2.34
	O4	-1.02	-2.22	0.04	2.44
	O'4	1.06	2.03	0.45	2.33
	O9	-1.92	-0.47	-1.75	2.64

Table 3: Experimentally determined Hamiltonian parameters for Mn^{2+}substituted in sites Cal, Ca2, and Ca3

$g_1 = g_2 = 2.002$	$g_3 = 1.998$
$A_1 = A_2 = 85$ cm^{-1}	$A_3 = 8$ T cm^{-1}
$D_1 = D_2 = -357$ cm^{-1}	$D_3 = -231$ cm^{-1}
$E_1 = E_2 = 90$ cm^{-1}	$E_3 = 19$ cm^{-1}

The parameters $B^0{}_2$ = D/3 and $B^2{}_2$ = E of the axial and rhombic crystal fields, respectively, are experimentally determined by fitting the Hamiltonian (1) to the ESR spectra. These two terms can be calculated as functions of the charge of the ligands, and using the expressions for A^m given by Poole and Farach (1987) in terms of the Tesseral harmonics we get

$$\frac{g^2\beta^2}{2}\left\langle\frac{r^2-3x^2}{r^5}\right\rangle = -\frac{1}{3}D + E \quad (4)$$

$$\frac{g^2\beta^2}{2}\left\langle\frac{r^2-3y^2}{r^5}\right\rangle = -\frac{1}{3}D - E \quad (5)$$

$$\frac{g^2\beta^2}{2}\left\langle\frac{r^2-3z^2}{r^5}\right\rangle = \frac{2}{3}D \quad (6)$$

The results of these calculations are presented in Table 2, from which we can determine the ratios between the E and D parameters for Mn^{2+} at the Ca sites Cal, Ca2, and Ca3:

$$\left|\frac{E_1}{D_1}\right| = \left|\frac{E_2}{D_2}\right| = 0.15 \quad (7)$$

$$\left|\frac{E_3}{D_3}\right| = 0.12$$

Computer Fit to Spectrum

The next step was to write a computer program to generate the theoretical spectrum for different orientations of the applied magnetic field and, by trial and error, to make a fitting to our experimental spectra. In this computer program we used the Hamiltonian given by Equation 1 and followed the procedure given by Bird (1964) [1] to express the energies to third-order perturbation and the probability of a transition from the state $|M, m\rangle$ to the state $|M', m\rangle$ under the action of a microwave field.

By comparing the theoretical spectrum generated by the computer program for the maximum spread (Fig. 4) with the experimental one, we find that the Hamiltonian parameters for the two kinds of sites for wollastonite are as listed in Table 3. Thus, g and A are isotropic, and the angular dependence arises

entirely from the D and E terms. These parameters explain the dependence of the ESR spectrum on the orientation of the applied magnetic field. From the above values, the measured ratios $|E_1/D_1| = |E_2/D_2|$ and $|E_3/D_3|$ are, respectively, 0.25 and 0.08, which give a reasonable agreement with those calculated by crystal field theory.

Discussion

It was mentioned above that the sample being examined contained 5.7% calcite and 5.5% dolomite, both of which commonly incorporate Mn in Ca sites. The Ca sites in these two minerals have point symmetry C_{3i}, $\bar{3}$, and the presence of the three-fold axis causes the E term in the Hamiltonian to vanish. This result has been demonstrated experimentally by ESR studies that give the values D = 37.5, E = 0 for Mn in calcite (Hodges *et al*., 1968; Tennant, 1974); D = 76.5, E = 0 for Mn in calcite (Wildeman, 1970; Schindler and Ohose, 1969, 1970) [9]; D = 3, E = 0 for Mn in dolomite, Ca site (Wildeman, 1970; Schindler and Ghose, 1969, 1970) [9]; and D = 141.9, E = 0 for Mn in dolomite, Mg site (Wildeman, 1970; Schindler and Ghose, 1969, 1970) [9]. In this study no signal was detected with E = 0, which shows that the observed spectra were due to wollastonite and not to calcite or dolomite. The Ca sites in wollastonite have symmetry l, so a non-vanishing *E* term is expected, as observed. The lower symmetry of the Ca sites in wollastonite produces larger *D*-term values than those in calcite and dolomite.

Conclusion

The ESR spectrum in wollastonite is interpreted as originating from Mn^{2+} ions on two magnetically nonequivalent Ca sites. This interpretation is in agreement with the presence of three Ca sites (Cal, Ca2, and CA3) in wollastonite, two of which are 6-coordinated and one of which is 7-coordinated. Theoretical spectra that fit the experimental spectra of this study were generated by superposition of two calculated spectra generated according to Bird's procedure (Bird, 1964) [1]. These calculated spectra provide the Hamiltonian parameters for Mn24 given in Table 3. From a crystal-field calculation the respective ratios $|E_1/D_1| = |E_2/D_2| = 0.15$ and $|E_3/D_3| = 0.12$ were found for the two sites.

References

1. Bird GL. Intensity of allowed and forbidden electronic paramagnetic resonance lines. Soviet Physics—Solid State. 1964; 5:1628-1635.
2. Bleaney B. Hyperfine structure in paramagnetic salts and nuclear alignment. Philosophical Magazine. 1951; 42:441-458.
3. Buerger MJ, Prewitt CT. the crystal structure of wollastonite and pectolite. Proceedings of the National Academy of Sciences USA. 1961; 47:1884-1888.
4. Hodges JA, Marshall SA, McMillan JA, Serway RA. Superhyperfine interaction due to ^{13}C in the ESR absorption spectrum of Mn^{2+} in single-crystal calcite. Journal of Chemical Physics. 1968; 49:2857- 2858.
5. Ladoo RB. wollastonite in industrial minerals and rocks, SW. Mudd, Ed., American Institute of Mining and Metallurgy Engineers, 1937.
6. Mamedov KH, Belov NV. Crystal structure of wollastonite. Doklady Akademii Nauk SSSR. 1956; 107:463-466.
7. Peacor DR, Prewitt CT. Comparison of the crystal structures of bustamite and wollastonite. American Mineralogist. 1963; 48:588-596.
8. Poole CP, Farach HA. the theory of magnetic resonance (2nd edition). Wiley-Interscience, New York, 1987.
9. Schindler P, Ghose S. Electron paramagnetic resonance of Mn^{2+} in dolomite, Ca Mg $(Co_3)_2$ and magnesite, $MgCo_3$, and Mn^{2+} distribution in dolomites (abs.). Transactions of the American Geophysical Union. 1969; 50:357.
10. Electron paramagnetic resonance of Mn^{2+} in dolomite and magnesite, and Mn^{2+} distribution in dolomites. American Mineralogist. 1970; 55:1889-1896.
11. Tennant WC. Forbidden" lines in the ESR of Mn^{2+} in calcite. Journal of Magnetic Resonance. 1974; 14:152-159.